

STRANGE BEAUTY AND OTHER BEASTS FROM $\Upsilon(5S)$ AT BELLE ^a

K. Kinoshita

*University of Cincinnati, PO Box 210011
Cincinnati, OH 45221, USA*

The B -factories have successfully exploited the unique advantages of the $\Upsilon(4S)$ resonance to study many aspects of B_d and B_u mesons. The $\Upsilon(10860)$ (aka $\Upsilon(5S)$) resonance, which is above mass threshold for the B_s and shares many of the same advantages, has been relatively unexplored. The Belle experiment has collected more than 120 fb^{-1} at the $\Upsilon(10860)$ and 7.9 fb^{-1} at higher energies, corresponding to more than 7 million B_s events. Recent results based on $\approx 20\%$ of these data are presented and prospects for future possibilities discussed.

The Belle experiment,¹ located at KEKB,² was built primarily to measure CP asymmetries of B meson decay in e^+e^- annihilations at the $\Upsilon(4S)$ resonance. In December 2009, the integrated luminosity surpassed 1000 fb^{-1} ($=1 \text{ ab}^{-1}$), fulfilling the goal stated in the original Belle proposal. Not all of the data were taken at the $\Upsilon(4S)$, however – results from the $\Upsilon(10860)$ resonance are presented here.

The $\Upsilon(10860)$, ($Mc^2 = 10865 \pm 8 \text{ MeV}/c^2$, $\Gamma = 110 \pm 13 \text{ MeV}$),³ is interpreted as $\Upsilon(5S)$, the fourth excitation of the vector bound state of $b\bar{b}$. It is above $B_s\bar{B}_s$ threshold and, given the success of the $\Upsilon(4S)$ program in characterizing properties of $B_{d,u}$, it is natural to contemplate B_s at $\Upsilon(10860)$. The e^+e^- environment produces clean events, efficiently triggered, with precisely known center-of-mass energy. Furthermore, the B -factory offers an existing facility with high luminosity, a well-studied detector with precise and sensitive photon detection, and an abundance of $\Upsilon(4S)$ data for comparisons. While rates are low compared to hadronic collisions, $\sigma(e^+e^- \rightarrow \Upsilon(10860)) \approx \sigma(e^+e^- \rightarrow \Upsilon(4S))/3 \approx 0.3 \text{ nb}$, and events include $B_{d,u}$ as well as B_s , the $\Upsilon(10860)$ can be competitive nonetheless, particularly in aspects of B_s decay that are limited by systematic effects at a hadron machine.

Belle has collected data at the $\Upsilon(10860)$ in several runs. In June 2005 a three-day “engineering” run served to test KEKB, which had never operated at energies above the $\Upsilon(4S)$, and study the basics of $\Upsilon(10860)$, B_s , and B_s^* . A scan of five energy points was used to locate the peak, at $\sqrt{s} = 10869 \text{ MeV}$, where 1.86 fb^{-1} were collected. By June 2006, results confirmed the projected potential of $\Upsilon(10860)$, and 21.7 fb^{-1} were collected in 20 days. In December 2007, $\approx 8 \text{ fb}^{-1}$ were collected in a scan of six energy points near and above the $\Upsilon(10860)$. Finally, a large fraction of the data collected in October 2008–December 2009 have been at the resonance. The integrated luminosity collected on resonance over all data sets thus far is $\approx 120 \text{ fb}^{-1}$.

As prerequisite to studies of B_s , its abundance in $\Upsilon(10860)$ events was determined from the 2005 data.⁴ About 10% of the hadronic events are resonance (assumed to be $b\bar{b}$), the rest being continuum $e^+e^- \rightarrow q\bar{q}$ ($q = u, d, s, c$). Figure 1 (L) displays R_2 , the ratio of the 2nd and 0th Fox-Wolfram moments,⁵ a measure of “jettiness” that tends to be lower for the more isotropic resonance events. We find $(3.01 \pm 0.02 \pm 0.16) \times 10^5 \text{ } b\bar{b} \text{ events}/\text{fb}^{-1}$. The $b\bar{b}$ events may fragment to: $B_s^{(*)}\bar{B}_s^{(*)}$, $B_q^{(*)}\bar{B}_q^{(*)}$, $B_q\bar{B}_q^{(*)}\pi$, $B_q\bar{B}_q\pi\pi$ (q is a u - or d -quark). The fraction (f_s) that are

^atalk presented at the XLVth Rencontres de Moriond, 6-13 March, 2010

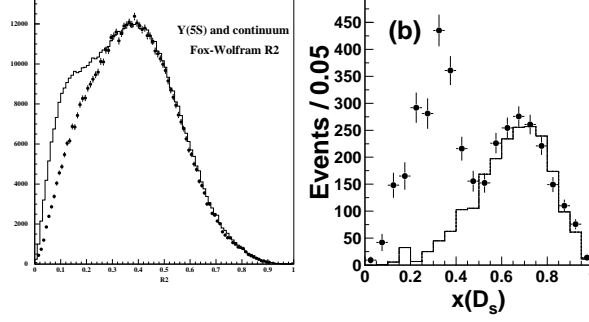


Figure 1: (L) Distribution in R_2 , (histogram) 1.86 fb^{-1} at the $\Upsilon(10860)$ and (points) continuum below $\Upsilon(4S)$, scaled. (R) Distribution of D_s in $x \equiv p_{D_s}/\sqrt{E_{beam}^2 - M_{D_s}^2}$, (points) $\Upsilon(10860)$ and (histogram) scaled continuum.

$B_s^{(*)}\bar{B}_s^{(*)}$ is determined through measurement of the inclusive rate $\mathcal{B}(\Upsilon(10860) \rightarrow D_s X) \equiv \mathcal{B}_\Upsilon$ (Figure 1(R)), an average over B_s , B_d , and B_u weighted by abundance, combined with the rate for $B_{u,d} \rightarrow D_s X$ measured at the $\Upsilon(4S)$ and a semi-theoretical estimate $\mathcal{B}(B_s \rightarrow D_s X) = (92 \pm 11)\%$,⁷ under an assumption that B_d and B_u are produced equally and that non- B production is negligible. The inclusive D^0 rate gives an independent value of f_s with larger uncertainties; $\mathcal{B}(B_s \rightarrow D^0 X) \ll \mathcal{B}(B_q \rightarrow D^0 X)$. The results are combined to obtain $f_s = (18.0 \pm 1.3 \pm 3.2)\%$.⁴

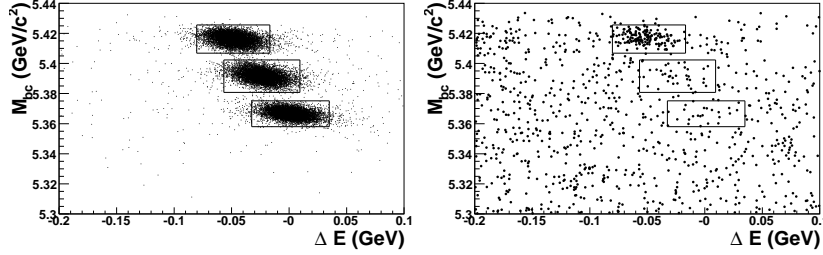


Figure 2: Illustration of full reconstruction method, $B_s \rightarrow D_s \pi$. Distributions in ΔE and M_{bc} of candidates, (Left) Monte Carlo simulation, (Right) data, 23.6 fb^{-1} . Also shown are signal regions for $B_s^*\bar{B}_s^*$ (upper signal box), $B_s^*\bar{B}_s$ (middle box), and $B_s\bar{B}_s$ (lower box) events.

At the energy of the $\Upsilon(10860)$, three types of B_s events are allowed: B_s pairs, B_s^* pairs, and mixed $B_s\bar{B}_s^*$ events. These three types may be separated through “full reconstruction” of B_s decays, where all decay products are measured, a method used with great success for B_q at the $\Upsilon(4S)$. Each candidate’s energy and momentum in the e^+e^- center-of-mass are evaluated as $\Delta E \equiv E_{cand} - E_{beam}$ and $M_{bc} \equiv \sqrt{E_{beam}^2 - p_{cand}^2}$. In $B_s\bar{B}_s$ events (analogous to $\Upsilon(4S) \rightarrow B_q\bar{B}_q$), the B_s carries the beam energy, so $\langle \Delta E \rangle = 0$ and $\langle M_{bc} \rangle = M_{B_s}$. For $B_s^*\bar{B}_s$ or $B_s^*\bar{B}_s^*$, the kinematics of $B_s^* \rightarrow B_s \gamma$ ($E_\gamma = 50 \text{ MeV}$) leads to localized signals as well. In the case of $B_s^*\bar{B}_s$ the end result is effectively the loss of 50 MeV from the B_s pair, with the energy difference being shared approximately equally: $\langle \Delta E \rangle \approx -25 \text{ MeV}$ and $\langle M_{bc} \rangle \approx M_{B_s} + 25 \text{ MeV}$. For $B_s^*\bar{B}_s^*$ the corresponding energy reduction is $\sim 50 \text{ MeV}$. Figure 2 shows distributions in ΔE and M_{bc} for $B_s \rightarrow D_s^- \pi^+$ candidates, signal Monte Carlo simulations and (previously reported) data.⁶ The B_s yields are extracted from a two-dimensional fit in these two variables, unless otherwise specified. From the relative yields of the three modes, we find⁶

$$f_{B_s^*B_s^*} \equiv \frac{\sigma(e^+e^- \rightarrow B_s^*\bar{B}_s^*)}{\sigma(e^+e^- \rightarrow B_s^{(*)}\bar{B}_s^{(*)})} = (90.1^{+3.8}_{-4.0} \pm 0.2)\%$$

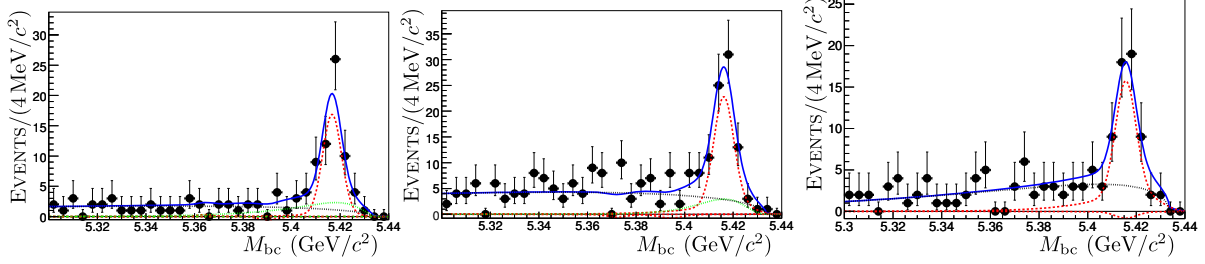


Figure 3: Projections in M_{bc} for 23.6 fb $^{-1}$ data: (left) $B_s \rightarrow D_s^* \pi$, (center) $B_s \rightarrow D_s \rho$, (right) $B_s \rightarrow D_s^* \rho$.

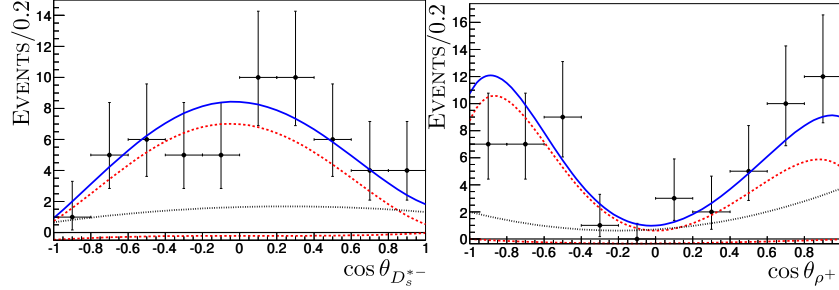


Figure 4: Projections in helicity angles of $B_s \rightarrow D_s^* \rho$ signal events: (left) $\cos \theta_{D_s^*-}$, (right) $\cos \theta_{\rho^+}$.

$$f_{B_s^* B_s} \equiv \frac{\sigma(e^+ e^- \rightarrow B_s^* \bar{B}_s + B_s \bar{B}_s^*)}{\sigma(e^+ e^- \rightarrow B_s^{(*)} \bar{B}_s^{(*)})} = (7.3 \pm 0.3 \pm 0.1)\%$$

The new results presented here, based on 23.6 fb $^{-1}$ of data collected in 2005-6, include $B_s \rightarrow D_s^{*-} \pi^+$, $D_s^{(*)-} \rho^+$, $B_s \rightarrow D_s^{(*)+} D_s^{(*)-}$, $B_s \rightarrow J/\psi \eta^{(\prime)}$, $B_s \rightarrow hh$, and $\Upsilon(5S) \rightarrow B \bar{B} X$.

The decays $B_s \rightarrow D_s^{(*)-} h^+$, where h is a light non-strange meson, proceed dominantly via a CKM-favored spectator process. We reconstruct D_s in the modes $\phi(\rightarrow K^+ K^-) \pi^-$, $K^{*0}(\rightarrow K^+ K^-) K^-$, and $K_S(\rightarrow \pi^+ \pi^-) K^-$. Shown in Figure 3 are fits to data, projected into M_{bc} , for $B_s \rightarrow D_s^{*-} \pi^+$, $D_s^- \rho^+$, and $D_s^{*-} \rho^+$. Two-dimensional fitting for $B_s^* \bar{B}_s^*$ only yields signals $53.4^{+10.3}_{-9.4}$ (7.1 σ) and $92.2^{+14.2}_{-13.2}$ (8.2 σ) in $B_s \rightarrow D_s^{*-} \pi^+$ and $B_s \rightarrow D_s^- \rho^+$, respectively. Taking $f_{B_s^* B_s} = 90.1\%$, $f_s = (19.5^{+3.0}_{-2.3})\%$, and $\sigma_{e^+ e^- \rightarrow b \bar{b}} = 0.302 \pm 0.014$ nb (a weighted average from 4,8), we find $\mathcal{B} = (2.4^{+0.5}_{-0.4} \pm 0.3 \pm 0.4) \times 10^{-3}$ and $\mathcal{B} = (8.5^{+1.3}_{-1.2} \pm 1.1 \pm 1.3) \times 10^{-3}$.⁹ For each result, first error is statistical, the third is systematic (due to the uncertainty in f_s), and the second is systematic (from all other uncertainties). For $B_s \rightarrow D_s^{*-} \rho^+$, a pseudoscalar decay to two vectors, the distributions in the helicity angles $\theta_{D_s^{*-}}$ and θ_{ρ^+} depend on the relative contribution from the different helicity states, which depends on the detailed hadronization mechanism for the decay; for example, the factorization hypothesis predicts that longitudinal polarization dominates: $f_L \approx 88\%$.¹⁰ A four-dimensional fit yields $77.7^{+14.6}_{-13.3}$ (7.4 σ) signal events from which we derive a branching fraction $(11.8^{+2.2}_{-2.0} \pm 1.7 \pm 1.8) \times 10^{-3}$.⁹ We also measure $f_L = 1.05^{+0.08+0.03}_{-0.10-0.04}$.⁹

If the B_s decays via the spectator process where the W^- couples to $s \bar{c}$, the net flavor of the final state is zero: $c \bar{s} \bar{c} s$. If the b - and c -quark masses are infinite, $CP=+1$. Because the state is not far above mass threshold, two-body final states, $B_s \rightarrow D_s^{(*)-} D_s^{(*)+}$, are expected to dominate.¹¹ As the $s \bar{c}$ coupling is CKM-favored, this channel comprises a substantial fraction of B_s decay channels, of order 10%, resulting in a substantial asymmetry in lifetime between the two CP eigenstates that is related to the branching fraction for $B_s \rightarrow D_s^{(*)-} D_s^{(*)+}$: $\frac{\Delta \Gamma_{CP}}{\Gamma} \approx \frac{2\mathcal{B}(B_s \rightarrow D_s^{(*)+} D_s^{(*)-})}{1 - \mathcal{B}(B_s \rightarrow D_s^{(*)+} D_s^{(*)-})}$.¹³ The quantity of interest here is the sum, which is difficult to measure at

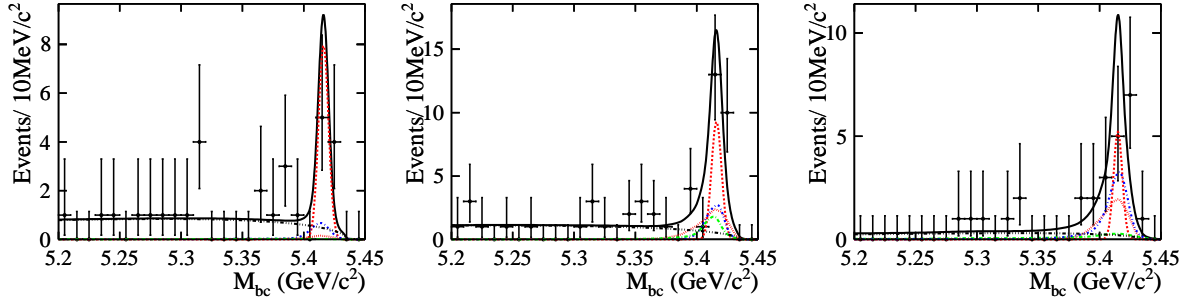


Figure 5: Projections in M_{bc} , based on 23.6 fb^{-1} of Belle data at $\Upsilon(10860)$: (left) $B_s \rightarrow D_s^+ D_s^-$, (center) $B_s \rightarrow D_s^{*+} D_s^-$, (right) $B_s \rightarrow D_s^{*-} D_s^{*+}$ curves show the fitted total (blue), signal (dashed), wrong combination (dotted; red), cross-feed (dash-dotted; blue), combinatorial (dash-3dot).

Table 1: Yields, branching fractions, and signal significance for $B_s \rightarrow D_s^{(*)-} D_s^{(*)+}$.

Mode	Yield	$\mathcal{B}(\%)$	S
$D_s^- D_s^+$	$8.5^{+3.2}_{-2.6}$	$1.0^{+0.4+0.3}_{-0.3-0.2}$	6.2
$D_s^- D_s^{*+}$	$9.2^{+2.8}_{-2.4}$	$2.8^{+0.8}_{-0.7} \pm 0.7$	6.6
$D_s^{*-} D_s^{*+}$	$4.9^{+1.9}_{-1.7}$	$3.1^{+1.2}_{-1.0} \pm 0.8$	3.2

hadron machines due to low efficiencies for detection of the photon from $D_s^* \rightarrow D_s \gamma$.

We reconstruct $B_s \rightarrow D_s^{(*)-} D_s^{(*)+}$ candidates in the following modes: $D_s^{*+} \rightarrow D_s^+ \gamma$; $D_s^+ \rightarrow \phi \pi^+$, $K_S^0 K^+$, $\bar{K}^{*0} K^+$, $\phi \rho^+$, $K^{*+} K_S^0$, $K^{*+} \bar{K}^{*0}$; $\phi \rightarrow K^+ K^-$; $K_S^0 \rightarrow \pi^+ \pi^-$; $\bar{K}^{*0} \rightarrow K^- \pi^+$; $\rho^+ \rightarrow \pi^+ \pi^0$; $K^{*+} \rightarrow K_S^0 \pi^+$. Candidates are pre-selected by requiring $5.2 < M_{bc} c^2 / \text{GeV} < 5.45$ and $-0.15 < \Delta E / \text{GeV} < 0.1$. In each event the candidate with the lowest χ^2 based on $M(D_s)$ and $M(D_s^*) - M(D_s)$ is selected. The yield is evaluated through a simultaneous fit, over all three modes $B_s \rightarrow D_s^{(*)-} D_s^{(*)+}$, accounting for signal, combinatorial background, crossfeed from the other signal modes, and wrong combinations in signal events. Projections onto M_{bc} are shown in Figure 5 and the yields and branching fractions in Table 1. Taking the sum, $\mathcal{B} = 6.9^{+1.5}_{-1.3} \pm 1.9$, we calculate $\frac{\Delta \Gamma_{CP}}{\Gamma} = 0.147^{+0.036+0.044}_{-0.030-0.042} \pm 0.004$, where the last error is the estimated theory error. This value is consistent with the current PDG value, $0.092^{+0.051}_{-0.054}$.

In the Standard Model, mixing-mediated CP -violation occurs in neutral mesons due to the complex argument of the product of CKM matrix elements of the mixing “box diagram.” For B_s the relevant product is $V_{tb}^{*2} V_{ts}^2$, which is real, so that no significant asymmetry is expected. CP -asymmetries in decays of B_s thus present an opportunity to reveal New Physics. These measurements will require the reconstruction of a sizable sample of CP -defined final states.

The decays $B_s \rightarrow J/\psi \eta^{(\prime)}$ ($CP = +1$) proceed by the same process as the $B \rightarrow J/\psi K^0$, so the branching fractions may be estimated based on the measured $\mathcal{B}(B_d^0 \rightarrow J/\psi K^0) = 8.71 \times 10^{-4}$: $\mathcal{B}(B_s \rightarrow J/\psi \eta) \approx 3.5 \times 10^{-4}$, $\mathcal{B}(B_s \rightarrow J/\psi \eta') \approx 4.9 \times 10^{-4}$. The decays are reconstructed in the following modes: $J/\psi \rightarrow e^+ e^-$, $\mu^+ \mu^-$; $\eta \rightarrow \gamma \gamma$, $\pi^+ \pi^- \pi^0$; $\eta' \rightarrow \eta \pi^+ \pi^-$, $\rho^0 \gamma$. The signals are extracted via a 2-dimensional fit in ΔE and M_{bc} . A yield of 14.9 ± 4.1 events (7.3σ) is observed in the channel $B_s \rightarrow J/\psi \eta$; projections in M_{bc} are shown in Figure 6. We measure $\mathcal{B}(B_s \rightarrow J/\psi \eta) = (3.32 \pm 0.87(\text{stat})^{+0.32}_{-0.28}(\text{sys}) \pm 0.42(f_s)) \times 10^{-4}$ and $\mathcal{B}(B_s \rightarrow J/\psi \eta') = (3.1 \pm 1.2(\text{stat})^{+0.5}_{-0.6}(\text{sys}) \pm 0.4(f_s)) \times 10^{-4}$.

We have also searched for the CP -eigenstate modes $B_s \rightarrow K^+ K^-$, $B_s \rightarrow K^0 \bar{K}^0$, and $B_s \rightarrow \pi^- \pi^+$, as well as the flavored mode $B_s \rightarrow K^- \pi^+$. We find $\mathcal{B}(B_s \rightarrow K^+ K^-) = (3.8^{+1.0}_{-0.9}(\text{stat}) \pm 0.5 \pm 0.5(f_s)) \times 10^{-5}$, $\mathcal{B}(B_s \rightarrow K^0 \bar{K}^0) < 6.6 \times 10^{-5}$ (90% CL), $\mathcal{B}(B_s \rightarrow K^- \pi^+) < 2.6 \times 10^{-5}$ (90% CL), $\mathcal{B}(B_s \rightarrow \pi^- \pi^+) < 1.2 \times 10^{-5}$ (90% CL). The findings for $K^+ K^-$ and $K^0 \bar{K}^0$ are the first

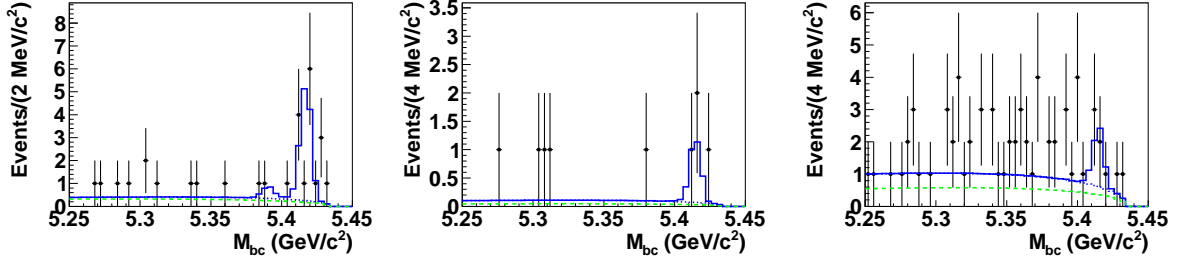


Figure 6: Projections in M_{bc} , based on 23.6 fb^{-1} of Belle data at $\Upsilon(10860)$: (left) $B_s \rightarrow J/\psi \eta$, (center) $B_s \rightarrow J/\psi \eta', \eta' \rightarrow \eta \pi \pi$, (right) $B_s \rightarrow J/\psi \eta', \eta' \rightarrow \rho \gamma$.

absolute branching fraction and first reported limit, respectively.

While B_s has been the main focus of studies at $\Upsilon(10860)$, the well-tuned methods of B reconstruction at the $\Upsilon(4S)$ may be applied to study the more complicated assortment of B events at the $\Upsilon(10860)$.¹² The relative rates may inform us about hadronization dynamics, and the total rate is needed to account for all $b\bar{b}$ events. Neutral and charged B 's are reconstructed in the following modes and submodes: $B^+ \rightarrow J/\psi K^+$, $\bar{D}^0 \pi^+$; $B^0 \rightarrow J/\psi K^{*0}$, $D^- \pi^+$; $J/\psi \rightarrow e^+ e^-$, $\mu^+ \mu^-$; $K^{*0} \rightarrow K^+ \pi^-$; $\bar{D}^0 \rightarrow K^+ \pi^-$, $K^+ \pi^+ \pi^- \pi^-$; $D^- \rightarrow K^+ \pi^- \pi^-$. As with the fully reconstructed B_s , the signal events populate the $(\Delta E, M_{bc})$ plane in clusters depending on the type of event. Figure 7(left) shows the projections in M_{bc} of the distributions for the various event types. The distribution of candidates in data, after background subtraction, are shown in Figure 7(right). While the distributions for events containing additional pions overlap each other, it is clear from data that their contribution is relatively small and that the majority of the rate is due to two-body events, $B^{(*)} \bar{B}^{(*)}$. It is also noted that there is an accumulation of events in the region of $B \bar{B} \pi \pi$, in the region of high M_{bc} . The fraction of $b\bar{b}$ events fragmenting to $B \bar{B}$, $B^* \bar{B}$, and $B^* \bar{B}^*$ are found to be $(5.5^{+1.0}_{-0.9} \pm 0.4)\%$, $(13.7 \pm 1.3 \pm 1.1)\%$, and $(37.5^{+2.1}_{-1.9} \pm 3.0)\%$, respectively. The events where M_{bc} is above the two-body limit are grouped together as “Large M_{bc} ” and found to comprise $(17.5^{+1.8}_{-1.6} \pm 1.3)\%$.

Multibody events, in which one or more additional pions is created, may be identified by pairing reconstructed B 's with additional charged pions in the event and examining the *residual* event energy and momentum, which correspond to the opposing $B^{(*)}$ and up to one additional pion. From the residual 4-momentum we reconstruct ΔE^{mis} and M_{bc}^{mis} . Projections onto M_{bc}^{mis} for various simulated event types are shown in Figure 8(left). The corresponding distribution in

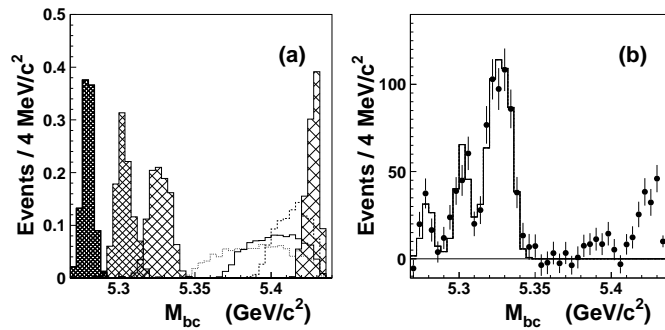


Figure 7: (a) MC simulated M_{bc} distributions for the $B^0 \rightarrow D^- \pi^+$ decay for $B \bar{B}$, $B \bar{B}^* + B^* \bar{B}$, $B^* \bar{B}^*$ and $B \bar{B} \pi \pi$ channels (cross-hatched histograms from left to right), and also for the three-body channels $B \bar{B}^* \pi + B^* \bar{B} \pi$ (plain histogram), $B \bar{B} \pi$ (dotted) and $B^* \bar{B}^* \pi$ (dashed). The distributions are normalized to unity. (b) M_{bc} distribution in data after background subtraction. The sum of the five studied B decays (points with error bars) and results of the fit (histogram) used to extract the two-body channel fractions are shown.

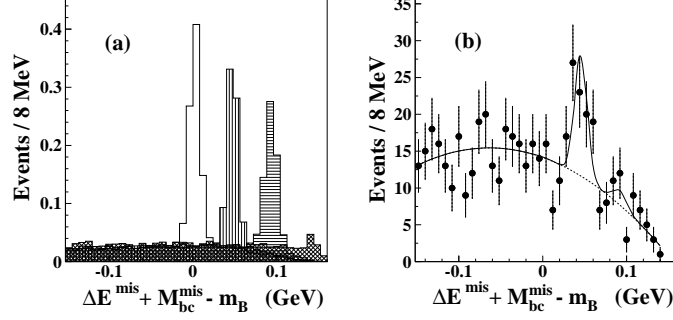


Figure 8: (a) The $\Delta E^{\text{mis}} + M_{\text{bc}}^{\text{mis}} - m_B$ distribution normalized per reconstructed B meson for the MC simulated $B^+ \rightarrow J/\psi K^+$ decays in the (peaks from left to right) $B\bar{B}\pi^+$, $B\bar{B}^*\pi^+ + B^*\bar{B}\pi^+$, $B^*\bar{B}^*\pi^+$, and $B\bar{B}\pi\pi$ channels. (b) The $\Delta E^{\text{mis}} + M_{\text{bc}}^{\text{mis}} - m_B$ data distribution for right-sign $B^{-/0}\pi^+$ combinations for all five studied B modes. The curve shows the result of the fit described in the text.

data, with fit result, is shown in Figure 8(right). The fractions of $b\bar{b}$ events to three-body modes $B\bar{B}\pi$, $B\bar{B}^*\pi$, and $B^*\bar{B}^*\pi$ are found to be $(0.0 \pm 1.2 \pm 0.3)\%$, $(7.3^{+2.3}_{-2.1} \pm 0.8)\%$, and $(1.0^{+1.4}_{-1.3} \pm 0.4)\%$, respectively. Paradoxically, no evidence for $B\bar{B}\pi\pi$ is observed, so this channel does not account for the remaining $(9.2^{+3.0}_{-2.8} \pm 1.0)\%$ of the “Large M_{bc} ” contribution observed in $\Upsilon(10860) \rightarrow BX$. The residual is quantitatively consistent with initial state radiation, $e^+e^- \rightarrow e^+e^-\gamma$, $e^+e^- \rightarrow b\bar{b}$, where about half the $b\bar{b}$ form the $\Upsilon(4S)$ resonance.

In summary the Belle experiment, which was designed to measure CP -asymmetry in B decay, is exploring the $\Upsilon(10860)$ resonance, with $\sim 120 \text{ fb}^{-1}$ data to date. We report on 23.6 fb^{-1} , ≈ 1.3 million B_s events. We have made first observations of $B_s \rightarrow D_s^{*-}\pi^+$, $D_s^{(*)-}\rho^+$, $B_s \rightarrow D_s^{*+}D_s^-$ and $B_s \rightarrow J/\psi\eta$. First evidence for $B_s \rightarrow D_s^{*+}D_s^{*-}$ and $B_s \rightarrow J/\psi\eta'$ are also reported, and search for $B_s \rightarrow hh$ has yielded first limits on $B_s \rightarrow K^0\bar{K}^0$. Using full reconstruction, we measure the rates for $\Upsilon(5S) \rightarrow BX$, $B\pi X$ and the fractions of $B_q^{(*)}\bar{B}_q^{(*)}$ and $B_q\bar{B}_q^{(*)}\pi$. We find a residual component of 9.2% which is consistent with being from initial state radiation.

Acknowledgments

The author wishes to thank the organizers and staff of the 45th Rencontres de Moriond. This work is supported by Department of Energy grant # DE-FG02-84ER40153.

1. Belle Collaboration, A. Abashian *et al.*, Nucl. Instr. Meth. A **479**, 117 (2002); Z. Natkaniec *et al.* (Belle SVD2 Group), Nucl. Instr. Meth. A **560**, 1 (2006).
2. S. Kurokawa and E. Kikutani, Nucl. Instrum. Meth., **A499**, 1 (2003), and other papers included in this Volume.
3. C. Amsler *et al.* (Particle Data Group), Physics Letters **B667**, 1 (2008) and 2009 partial update for the 2010 edition
4. A. Drutskoy *et al.* (Belle Collaboration), Phys. Rev. Lett. **98**, 052001 (2007).
5. G.C. Fox and S. Wolfram, Phys. Rev. Lett. **41**, 1581 (1978).
6. R. Louvot *et al.* (Belle collaboration), Phys. Rev. Lett. **102**, 021801 (2009).
7. M. Artuso *et al.* (CLEO Collaboration), Phys. Rev. Lett. **95**, 261801 (2005).
8. G.S. Huang *et al.* (CLEO Collaboration), Phys. Rev. **D 75**, 012002 (2007).
9. R. Louvot *et al.* (Belle collaboration), arXiv:1003.5312[hep-ex] Phys. Rev. Lett. in press.
10. J. L. Rosner, Phys. Rev. **D 42**, 3732 (1990).
11. I. Dunietz, R. Fleischer, and U. Nierste, Phys. Rev. **D63**, 114015 (2001) hep-ph/0012219.
12. A. Drutskoy *et al.* (Belle Collaboration), arXiv:1003.5885[hep-ex] submitted to Phys. Rev.

13. R. Aleksan et al., Phys. Lett. **B316**, 567 (1993).